

Bias-Exchange Metadynamics Simulations: An Efficient Strategy for the Analysis of Conduction and Selectivity in Ion Channels

Carmen Domene,^{†,‡} Paolo Barbini,[§] and Simone Furini^{*,§}

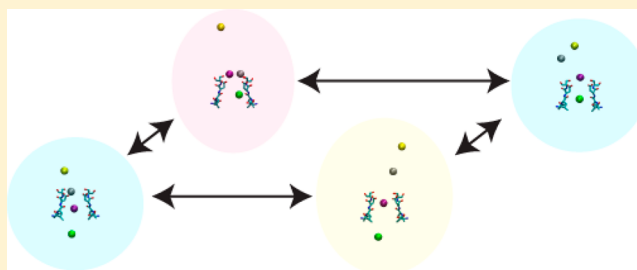
[†]Chemistry Research Laboratory, University of Oxford, 12 Mansfield Road, Oxford OX1 3TA, U.K.

[‡]Department of Chemistry, King's College London, Britannia House, 7 Trinity Street, London SE1 1DB, U.K.

[§]Department of Medical Biotechnologies, University of Siena, viale Mario Bracci 16, I-53100, Siena, Siena, Italy

S Supporting Information

ABSTRACT: Conduction through ion channels possesses two interesting features: (i) different ionic species are selected with high-selectivity and (ii) ions travel across the channel with rates approaching free-diffusion. Molecular dynamics simulations have the potential to reveal how these processes take place at the atomic level. However, analysis of conduction and selectivity at atomistic detail is still hampered by the short time scales accessible by computer simulations. Several algorithms have been developed to “accelerate” sampling along the slow degrees of freedom of the process under study and thus to probe longer time scales. In these algorithms, the slow degrees of freedom need to be defined in advance, which is a well-known shortcoming. In the particular case of ion conduction, preliminary assumptions about the number and type of ions participating in the permeation process need to be made. In this study, a novel approach for the analysis of conduction and selectivity based on bias-exchange metadynamics simulations was tested. This approach was compared with umbrella sampling simulations, using a model of a Na⁺-selective channel. Analogous conclusions resulted from both techniques, but the computational cost of bias-exchange simulations was lower. In addition, with bias-exchange metadynamics it was possible to calculate free energy profiles in the presence of a variable number and type of permeating ions. This approach might facilitate the definition of the set of collective variables required to analyze conduction and selectivity in ion channels.



INTRODUCTION

Ion channels are membrane proteins that control the fluxes of ions through cell membranes down their electrochemical gradients. They are classified into several families according to the ionic species that they are selective for (e.g., K⁺-channels, Na⁺-channels, or Ca²⁺-channels). Ion channels are key players in many biological processes, such as nerve transmission, muscular contraction, and cellular homeostasis, and, therefore, there is a notable interest in understanding how these proteins function at the atomic level. Although the first crystallographic structures of a K⁺ and a Na⁺-channel,^{1,2} solved in 1998 and 2011, respectively, represented remarkable breakthroughs in the field, crystal structures can only capture a steady state of a protein. In contrast, under physiological conditions, proteins will be dynamic and have a distinctive degree of flexibility. Therefore, to relate structural features with protein function, techniques such as Molecular Dynamics (MD) simulations, have been widely used, playing a critical role in the study of ion channels at the atomic level.³ Nonetheless, one of the major obstacles encountered with MD simulations in the study of biological processes is the time scales accessible by this technique, as most of the processes of interest in biology are usually remarkably long compared to the achievable time scales. A common strategy to probe longer time scales is to “accelerate” sampling along the slow degrees of freedom of the process

under investigation. These slow degrees of freedom are usually referred to as ‘reaction coordinates’ or ‘collective variables’. In the study of conduction and selectivity in ion channels, a natural choice for a collective variable could be the position of a permeating ion along the channel-axis. As conduction involves many ions, permeation is intrinsically an *N*-dimensional process, where *N* refers to the number of ions. This *N*-dimensional process could be described by *N* collective variables, each of which would track the movement of an ion along the pore. Once the choice of collective variables is established, several algorithms exist to maximize sampling and render the Potential of Mean Force (PMF). Among these algorithms, umbrella sampling (US) has been widely used in studies of ion conduction and selectivity.^{4–8} However, application of other approaches such as metadynamics,⁹ adaptive biasing force,¹⁰ or those based on the Jarzynski’s equality¹¹ have also been employed and reported in the literature recently. In all these algorithms, a set of collective variables describing the event of interest needs to be defined in advance, requiring the adoption of preliminary assumptions, e.g. the number and type of ions involved in conduction. Unfortunately, the optimal number of permeating ions might

Received: November 25, 2014

Published: March 5, 2015

be unknown, and it might also depend on various factors such as the concentration of ions and the membrane potential. For example, conduction in K⁺-channels was originally described as a two-ion process,⁴ but, subsequently, a conduction mechanism involving three ions was proposed on theoretical grounds⁵ in agreement with experimental predictions made by Hodgkin in the 1950s.¹² Similarly, conduction in Na⁺-selective channels has been described both in terms of two- or three-ion conduction events.^{6,9,13–15} In order to estimate by US the PMF profiles of permeation when different numbers of ions are involved, independent sets of simulations are required. In each of these sets, the number of collective variables is determined by the number of permeating ions that is considered in the process. In a situation where only one particular conduction mechanism is energetically relevant, the remaining sets of simulations would not be of much use, with the consequent misuse of computational resources. Besides, if several permeation mechanisms coexist, none of the independent simulation sets would provide the exact PMF profile; in each simulation, the system would be confined to a predefined region of the configurational space predetermined by the number of ions considered, while the real PMF would be the weighted average over all the possible trajectories connecting the initial and the final states of the permeation events.

In principle, ion permeation through a membrane protein could be characterized in a simulation that is “accelerated” along a single collective variable describing the movement of an ion crossing the permeation pore. In an infinite long simulation, ions not accelerated by biasing potentials would achieve equilibrium under the field of the ion tracked by the collective variable considered, or, in other words, the PMF would converge to the one experienced by the tracked-ion in the presence of the other ions of the system. However, if just one collective variable is taken into consideration, only the dynamics along that particular collective variable are accelerated and not the other degrees of freedom. The consequence is that the convergence of the PMF profile would be extremely slow, irrespective of the algorithm adopted to accelerate sampling. Unless the dynamics of the remaining ions in the system is also accelerated, convergence of this 1-dimensional PMF profile would not improve.

Estimating the PMF profile along one (or a few) collective variable(s), while at the same time accelerating sampling over a larger set of degrees of freedom is at the heart of bias-exchange metadynamics (BE-meta) simulations.¹⁶ In BE-meta, several replicas of the system are simulated in parallel. A metadynamics¹⁷ simulation is performed for each replica using a limited set of collective variables (usually one or two). In metadynamics, a history dependent potential that compensates for the underlying free energy surface along the biased collective variables is added to the potential energy of the system. As a consequence, the system is forced to escape local energy minima and to explore the space of the collective variables. In BE-meta simulations, each replica is biased along different collective variables, and at fixed time intervals exchanges between replicas are attempted. The atomic coordinates of two replicas (x_1 and x_2) are exchanged if replica swapping decreases the total biasing potential ΔV

$$\Delta V = (V_1(x_2) - V_1(x_1)) + (V_2(x_1) - V_2(x_2)) \quad (1)$$

where V_1 and V_2 are the biasing potentials in the two replicas. In the opposite situation, when the exchange of replicas results in an increase of ΔV , the swap is accepted with a probability

equal to $\exp(-\beta\Delta V)$, with β being the inverse temperature. In this way, the dynamics along the biased collective variable(s) in a certain replica is accelerated by the metadynamics biasing potential, and swapping configurations between replicas improves sampling along the collective variables biased by the whole set of simulations. Thus, by adopting this strategy, permeation of one ion per replica can be accelerated at the same time as sampling of the multidimensional configurational space defined by the remaining ions. Since ions can leave or remain inside the pore of the channel, the number of ions taking part in conduction can also vary.

In this manuscript, BE-meta and US simulations have been employed and compared in the study of ion conduction in a simplified model of a Na⁺-selective channel. Analogous results were obtained with both techniques, although BE-meta was computationally more efficient, with two key advantages: (i) the number and the type of ions involved in conduction events did not need to be predefined and (ii) conduction events where different number of ions are involved could be analyzed and compared using a unique simulation.

METHODS

Molecular System. The atomic model was based on the experimental structure of the bacterial Na⁺-channel NaVAb (Protein Data Bank entry 3RVY).² The system included the P-loop region of NaVAb, from residue Glu154 to Tyr193 (Figure S1 in the Supporting Information), solvated in a box of ~8,000 water molecules. N- and C-termini were amidated and acetylated, respectively. Default protonation states were used for protein residues. A total of 12 Na⁺ ions were added to achieve electrical neutrality. The protocol to equilibrate the system was 10,000 steps of energy minimization with the steepest descent algorithm, followed by 0.5 ns of dynamics in the NVT ensemble, and 1.5 ns in the NpT ensemble, with harmonic restraints applied to the heavy atoms of the protein (force constant equal to 2.19 kcal·mol⁻¹·Å⁻²). Subsequently, a 100 ns MD trajectory in the NpT ensemble was produced with harmonic restraints applied to the heavy atoms of residues 154 to 173 and 181 to 193 (force constant equal to 1.19 kcal·mol⁻¹·Å⁻²). These restraints were designed to preserve the architecture of the P-loop region in this simplified model. The residues of the selectivity filter, i.e. the region of the channel responsible for selective conduction of Na⁺ ions, were unrestrained.

MD simulations were performed with GROMACS version 4.5.5.¹⁸ The CHARMM27 force field with CMAP corrections was used for the protein,¹⁹ together with the TIP3P model for water molecules.²⁰ The Lennard-Jones parameters for Na⁺ and K⁺ ions were respectively $\epsilon = 0.0469$ kcal/mol and $R_{\min/2} = 1.36375$ Å and $\epsilon = 0.0870$ kcal/mol and $R_{\min/2} = 1.76375$ Å.²¹ Temperature was set to 300 K and controlled by velocity rescaling with stochastic terms (coupling time constant set to 0.1 ps).²² A pressure of 1 bar was imposed by coupling to a Parinello-Rahman barostat with a coupling time constant of 2 ps.²³ Electrostatic interactions were calculated with the Particle Mesh Ewald algorithm²⁴ with a maximum grid spacing for the Fourier transform of 1.2 Å. van der Waals interactions were truncated at 12 Å. Bond lengths were restrained with the LINCS algorithm.²⁵ The leapfrog algorithm was used to integrate the equations of motion using a time step of 2 fs.

Bias-Exchange Metadynamics (BE-Meta) Simulations. BE-meta simulations were performed with Plumed (version 1.3)²⁶ and GROMACS (version 4.5.5)¹⁸ using a different

number of replicas. In each BE-meta simulation, the number of replicas was set equal to the maximum number of ions considered in a permeation event, plus a “neutral” replica. The neutral replica is a simulation that swaps configurations with the other replicas but that is not affected by any time-dependent biasing potential. Sampling in the neutral replica approximates the equilibrium distribution with an accuracy that improves with slow-changing biasing potentials. The remaining replicas were biased using a time-dependent metadynamics potential that acted on a 1-dimensional collective variable (CV). This CV was defined as the distance along the channel-axis between an ion and the center of mass of the carbonyl oxygen atoms of residues Thr175 (intracellular entrance of the selectivity filter). Gaussians hills with height equal to 6×10^{-3} kcal/mol and width equal to 2.5×10^{-3} Å were added to the biasing potential every 2 ps. Exchanges between replicas were attempted every 50 ps. The biasing potential acted on a different ion in each replica, and, as a consequence, as the simulation proceeds, the biasing potential of each replica provided an estimate of the PMF experienced by the ion biased in that replica in the presence of the other ions of the system. The PMF for the i th replica (A_i) was estimated as

$$A_i(z_i) = -\frac{1}{\Delta t} \int_{t_{eq}}^{t_{eq}+\Delta t} V_i(z_i, t) dt \quad (2)$$

In eq 2, V_i is the biasing potential in the i th replica, z_i is the value of the collective variable for the ion accelerated by this biasing potential; t_{eq} is the equilibration time required to explore the entire CV space; and Δt is a time interval used to average out the oscillations of the biasing potential. In order to have control over the maximum number of ions inside the channel, the distance from the channel-axis of all the cations in the system was restricted by half-harmonic potentials. The distance from the channel-axis was measured as the distance in the xy -plane between the ion and the center of mass of the carbonyl oxygen atoms of residues Thr175 and Leu176. The half-harmonic potential was set to zero when the distance of the ion from the axis was lower than 8 Å, and it increased harmonically with force constant equal to $2.19 \text{ kcal} \cdot \text{mol}^{-1} \cdot \text{Å}^{-2}$ above this threshold, for all the ions biased by metadynamics potentials in any of the replicas. The remaining ions in the systems were excluded from permeation events by applying half-harmonic potentials that were equal to zero when the distance of the ion from the axis was higher than 8 Å and increased harmonically with a force constant equal to $2.19 \text{ kcal} \cdot \text{mol}^{-1} \cdot \text{Å}^{-2}$ below this threshold. Under these conditions, only ions accelerated by the biasing potentials were able to enter the protein pore.

In total, four BE-meta simulations were performed (Table 1) involving the following: (i) a neutral replica and two replicas with biasing potentials acting on the CV of two Na^+ ions

Table 1. BE-Meta Simulations^a

	1 st replica	2 nd replica	3 rd replica	4 th replica	t_{eq} (ns)
BE_2NA	Na^+ ion	Na^+ ion			50
BE_4NA	Na^+ ion	Na^+ ion	Na^+ ion	Na^+ ion	96
BE_2NA_1K	Na^+ ion	Na^+ ion	K^+ ion		136
BE_2NA_2K	Na^+ ion	Na^+ ion	K^+ ion	K^+ ion	152

^aIons biased in each replica in the BE-meta simulations. For each BE-meta simulation, the set of replicas included the ones listed in the table, plus a neutral replica with no biasing potential applied.

(BE_2NA); (ii) a neutral replica and four replicas with biasing potentials acting on the CV of four different Na^+ ions (BE_4NA); (iii) a neutral replica and three replicas with biasing potentials acting on the CV of two Na^+ ions and a K^+ ion (BE_2NA_1K); and (iv) a neutral replica and four replicas with biasing potential acting on the CV of two Na^+ ions and two K^+ ions (BE_2NA_2K).

Potential of Mean Force (PMF) Calculations. In order to estimate the PMF by eq 2, it is necessary to define an equilibration time, t_{eq} , and a time interval, Δt . For this purpose, the collective variable was discretized in bins of 0.5 Å, between -9 Å and $+29$ Å; this range corresponds to an ion moving from the intracellular to the extracellular compartment. t_{eq} was defined as the first time step when more than ten samples were collected for all the bins of the discretized collective variable in each replica of the BE-meta simulation. The time interval Δt was defined as $t_{eq}/2$. The rationale for this choice is the ability of the system to explore the entire range of the collective variable in a time interval t_{eq} , starting from a null-biasing potential. Thus, $t_{eq}/2$ is likely an overestimation of the time interval required to smooth out the oscillation of the biasing potentials.

Multidimensional PMF maps were calculated with the WHAM algorithm, using the procedure established by Marinelli et al. for BE-meta simulations.²⁷ The multidimensional space was discretized in cubic bins with each dimension set to 0.5 Å. First, the 1-dimensional PMF was calculated for each replica along the CV biased in that replica in time intervals $[t_{eq}, t_{eq}+\Delta t]$ and $[t_{eq}+\Delta t, t_{eq}+2\Delta t]$, and the two estimates were superimposed. The time interval $t_{eq}+2\Delta t$ corresponds to the total simulation time. For the WHAM calculations, only the configurations collected between the equilibration time (t_{eq}) and the total simulation time ($t_{eq}+2\Delta t$) were considered. In all the BE-meta simulations performed in this study, the maximum difference between the PMFs calculated by eq 2 in time intervals $[t_{eq}, t_{eq}+\Delta t]$ and $[t_{eq}+\Delta t, t_{eq}+2\Delta t]$ was lower than 1 kcal/mol. In the multidimensional PMF calculations, some of the collective variables actually described the same physical process. For instance, when a 2-dimensional PMF profile is calculated using simulation BE_2NA, the collective variables tracked in the two replicas describe the displacement along the channel axis of two (interchangeable) Na^+ ions. Therefore, a configuration with ions in $(z1, z2)$ is indistinguishable from one with ions in $(z2, z1)$. In order to increase the number of samples in each bin of the multidimensional grid, all the samples representing identical physical configurations (same type of ions but in different order) were combined to the one with $z1 < z2 < \dots < zN$. In the previous example, samples $(z1, z2)$ and $(z2, z1)$ are combined in the same bin, and the PMF is calculated only for the upper diagonal of the 2-dimensional space.

The 2-dimensional PMF map estimated from BE_2NA was compared with the PMF calculated from US simulations over the same region of the configurational space, using the same CVs. Identical radial restraints were imposed on the ions. The harmonic potentials in the US simulations were defined as follows:

$$\frac{k}{2}(CV_1 - CV_1^0)^2 + \frac{k}{2}(CV_2 - CV_2^0)^2 \quad (3)$$

The force constant k was set to $11.94 \text{ kcal} \cdot \text{mol}^{-1} \cdot \text{Å}^{-2}$. In eq 3, CV_1 and CV_2 are the values of the collective variable for two permeating ions; CV_1^0 and CV_2^0 are the corresponding centers of the harmonic potentials. The centers of the harmonic potentials

were translated with a step of 1.0 Å, and a trajectory of 2.1 ns was simulated for each configuration. The first 100 ps of each trajectory were considered as equilibration and discarded from further analyses. The PMF profile was calculated with the WHAM algorithm²⁸ over the same grid adopted for the BE-meta simulation.

Exploration of Estimated PMF Profile from the BE-Meta Simulation with Four Na⁺ Ions (BE_4NA). In order to identify metastable configurations and transitions pathways in the 4-dimensional PMF profile estimated from the BE-meta simulation BE_4NA (with four biased Na⁺ ions), Kinetic Monte Carlo (KMC) simulations were conducted using the Gillespie's algorithm.²⁹ The 4-dimensional space was discretized into microstates using the same grid adopted for the WHAM calculations (cubic bins with side equal to 0.5 Å). The transition rate between two adjacent microstates, i and j , was defined as

$$k_{i,j} = k_{i,j}^0 e^{-(1/2)\beta(F_j - F_i)} \quad (4)$$

where F_i and F_j are the PMF in the two microstates, β is the inverse temperature, and $k_{i,j}^0$ is the transition rate on a flat energy surface, which is a function of the diffusion coefficients along the CVs and the bins size.³⁰ The diffusion coefficients were assumed constant over the entire configurational space. Under these assumptions, i.e. the same ion diffusion coefficient inside and outside the channel, the transition rates $k_{i,j}^0$ only affect the time scale of the KMC trajectories but not the trajectories themselves.

In previous studies,^{6,13} two regions with high affinity for Na⁺ ions have been characterized in the selectivity filter of the NaVAb channel, and they were also confirmed using the model employed in this study (see Results section). These two regions correspond to a site close to the carbonyl oxygen atoms of residues Leu176 (biding site S_{CEN}) and a site close to the side chains of the charged residues Glu177 (binding site S_{HFS}). All possible configurations of four ions distributed over S_{CEN} (0.0 Å ≤ CV < 0.70 Å), S_{HFS} (0.70 Å ≤ CV ≤ 1.1 Å), and the extracellular (CV > 1.1 Å) and intracellular (CV < 0 Å) compartments were considered. Some of these configurations correspond to inaccessible states, e.g. four ions in the same binding site at the same time, or configurations with an empty pore. These configurations were never sampled in BE-meta simulations, and, consequently, their energy is undefined. For the remaining configurations, the Nelder–Mead³¹ minimization algorithm was used to find the position of the closest local energy minimum in the 4-dimensional space. Subsequently, 100 independent KMC trajectories were generated starting from each of the microstates in the 4-dimensional grid. A microstate was classified as part of the attraction basin of a local energy minimum if KMC trajectories starting from the microstate reached this minimum before any other local energy minimum in at least 90% of the cases. The energy of the basin was defined as the minimum energy of the microstates that belong to the basin. The energy barrier between two basins was defined as the minimum energy barrier encountered in KMC trajectories connecting the two basins; a KMC trajectory connects basin i to basin j if it goes from a microstate that is part of basin i to a microstate that is part of basin j without prior entrance in any state belonging to any other basins. The energy barriers between local minima were obtained from a KMC trajectory that sampled over 10⁶ basins transitions.

RESULTS

Simulations with Two Na⁺ Ions. The BE-meta simulation BE_2NA includes three replicas: the neutral replica, with no biasing potential applied, and two replicas in each of which the movement of an ion along the channel axis is biased (collective variable CV defined in the Methods section). Therefore, this set of simulations provides data on conduction events where one or two Na⁺ ions are involved. The positions of the ions accelerated by the biasing potentials explored the entire channel pore axis, from the intracellular to the extracellular side, in less than 50 ns in both replicas ($t_{eq} = 50$ ns). After this period, the PMF profile remains unchanged (Figure 1). This 1-dimensional

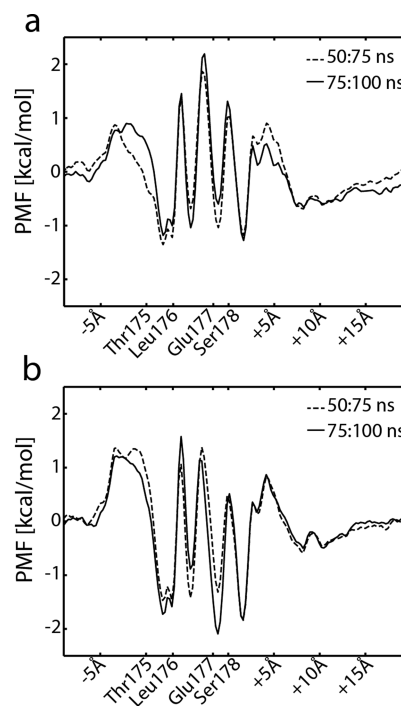


Figure 1. PMF of one Na⁺ ion in a BE-meta simulation with two Na⁺ ions. The PMF for the two replicas (panels a and b) was calculated by eq 2, in the time interval 50–75 ns (dashed line) and 75–100 ns (continuous line). In each replica, the biasing potential acted on the distance along the channel axis between a Na⁺ ion (a different ion for each replica) and the center of the carbonyl oxygens of residues Thr175. The labels along the x -axis indicate the average positions of the carbonyl oxygens of residues Thr175, Leu176, and Ser178 and of the side chain oxygens of residues Glu177. Displacements of -5 Å with respect to Thr175 (intracellular side of the selectivity filter) and $+5$ Å, $+10$ Å, and $+15$ Å with respect to Ser178 (extracellular side of the selectivity filter) are also shown.

PMF profile corresponds to the PMF experienced by one ion moving across the channel in the presence of the second ion. Four energy minima are clearly observed: two minima with an ion bound at the intracellular side of the pore, above or below the carbonyl oxygen atoms of residues Leu176 (S_{CEN}), and two minima close to the charged side chains of residues Glu177 (S_{HFS}). These PMF profiles are remarkably similar for the two replicas, and their difference gives an estimate of the uncertainty in the energy, which was found to be lower than 1 kcal/mol (Figure 2). Since the two replicas describe the same physical process, the similarity between the two estimates is somehow expected, and it confirms convergence of the BE-meta simulation.

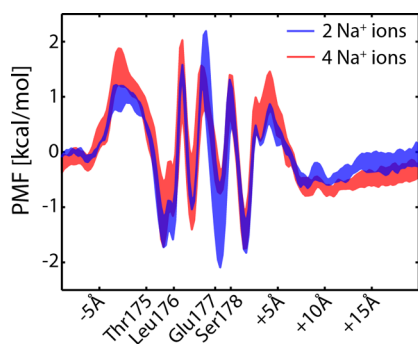


Figure 2. PMF of a Na^+ ion in BE-meta simulations with two Na^+ ions (in blue) or four Na^+ ions (in red). 1-dimensional PMF profiles are shown as the average of the PMF estimated in the various replicas, plus/minus the maximum distance among these different estimates (2 replicas in BE_2NA, 4 replicas in BE_4NA). The labels along the x -axis indicate the average positions of the carbonyl oxygen atoms of residues Thr175, Leu176, and Ser178 and of the side chain oxygen atoms of residues Glu177. Displacements of -5 Å with respect to Thr175 (intracellular side of the selectivity filter) and $+5$ Å, $+10$ Å, and $+15$ Å with respect to Ser178 (extracellular side of the selectivity filter) are also shown.

Although the 1-dimensional PMF profile defines clearly the ion binding sites and the energy barriers encountered by Na^+ ions across the pore, it does not reveal if conduction is a one- or two-ion process. To answer this question, it is necessary to explore conduction in a 2-dimensional space. The PMF map in a 2-dimensional space shows that single-ion conduction events are not achievable (Figure 3). All the energy minima correspond to configurations with at least one ion inside the protein pore. The lowest energy minimum corresponds to a situation with two ions at binding sites S_{CEN} and S_{HFS} , respectively. Conduction is likely to proceed as follows: $\text{IN}/S_{\text{CEN}} \rightarrow \text{IN}/S_{\text{HFS}} \rightarrow S_{\text{CEN}}/S_{\text{HFS}} \rightarrow S_{\text{CEN}}/\text{OUT}$, where IN and OUT correspond to an ion in the intracellular and extracellular compartment, respectively (see snapshots from the BE-meta simulations in the insets of Figure 3). The local energy minima appear as horizontal/vertical funnels in the 2-dimensional PMF map, which suggests that ion movements are largely independent from each other.

The energy profile shown in Figure 3 is similar to the one calculated by US using a model of the entire pore region of the NaVAb channel.¹³ The two energy profiles almost superimpose each other when the lower ion sits above residue Thr175. The differences that emerge when the first ion is below Thr175 are likely to be related to the nature of the experimental structure. The crystal structure of NaVAb corresponds to a closed conformation of the channel, while the simplified model adopted in this study is more likely to feature an open channel (inner helices that close the intracellular gate missing). The similarity between the PMF obtained from the two models suggests that the simplified model adopted in this study is a satisfactory representation of the selectivity filter region of a Na^+ channel.

For a direct comparison with well-established computational strategies, the 2-dimensional PMF was calculated also by US, using the same channel model. The force constant of the harmonic potentials in the US simulations was set to $11.94 \text{ kcal} \cdot \text{mol}^{-1} \cdot \text{\AA}^{-2}$, and the distance between adjacent simulations was set to 1.0 Å. These values are in the range usually reported in the literature, and they guarantee an adequate overlap between probability histograms of adjacent US simulations

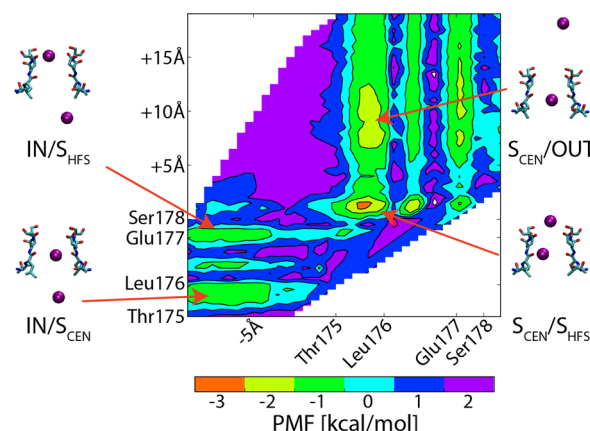


Figure 3. PMF in a BE-meta simulation with two Na^+ ions. The PMF was calculated with the WHAM algorithm, using data from the BE-meta simulation with two biased Na^+ ions (BE_2NA) in the time interval 50–100 ns. Labels along the axes indicate the average positions of the carbonyl oxygen atoms of residues Thr175, Leu176, and Ser178 and of the side chain oxygen atoms of residues Glu177. Displacements of -5 Å with respect to Thr175 (intracellular side of the selectivity filter) and $+5$ Å, $+10$ Å, and $+15$ Å with respect to Ser178 (extracellular side of the selectivity filter) are also shown. Contour lines are drawn every 1 kcal/mol. Snapshots of the selectivity filter from the BE-meta simulation are shown for configurations with ions in the intracellular compartment and the binding site S_{CEN} (IN/ S_{CEN}); the intracellular compartment and the binding site S_{HFS} (IN/ S_{HFS}); the binding sites S_{CEN} and S_{HFS} ($S_{\text{CEN}}/S_{\text{HFS}}$); and the binding site S_{CEN} and the extracellular compartment ($S_{\text{CEN}}/\text{OUT}$). Residues Thr175 to Ser178 of two subunits of the selectivity filter are shown in licorice representation. Sodium ions are shown as purple VdW spheres.

(choice of a higher distance between adjacent US simulations did not guarantee the overlap of histograms). The number of simulations needed to sample an identical or comparable 2-dimensional space from the BE-meta simulation was equal to 534. Figure 4a shows the average value of the difference between successive estimates of the 2-dimensional PMF map ($\langle |\Delta \text{PMF}| \rangle$) with US simulations of increasing length. In order to calculate the difference between two PMF profiles, the maps were first superimposed, and then ΔPMF was defined as the difference between the two maps. Changing the length of the US simulations from 250 to 500 ps modifies the PMF by ~ 0.5 kcal/mol on average (ΔPMF in the 2-dimensional space is shown in Figure S2 of the Supporting Information). A further increase from 500 to 750 ps modifies the PMF by an additional 0.2 kcal/mol. Therefore, US simulations of 500 ps seem to be too short to provide a converged PMF profile. Not surprisingly, the PMF map calculated with US simulations of this length differs from the one computed by the BE-meta simulation BE_2NA (Figure 4b). The two PMF maps are similar when the innermost ion (x -axis in Figures 3 and 4b) is inside the pore axis. Differences in energy higher than 3 kcal/mol emerge for configurations with the innermost ion in the intracellular compartment and the outermost ion inside the pore. These differences can be ascribed to the size of the US trajectories, e.g. 500 ps is not a long enough time to sample the equilibrium distribution of the CVs. A similar conclusion was reached in umbrella sampling simulations using a model of the entire pore region of the NaVAb channel.³² Noteworthy, US simulations of 500 ps (plus 100 ps of equilibration time per simulation) give a cumulative time of 320 ns, slightly higher than the time

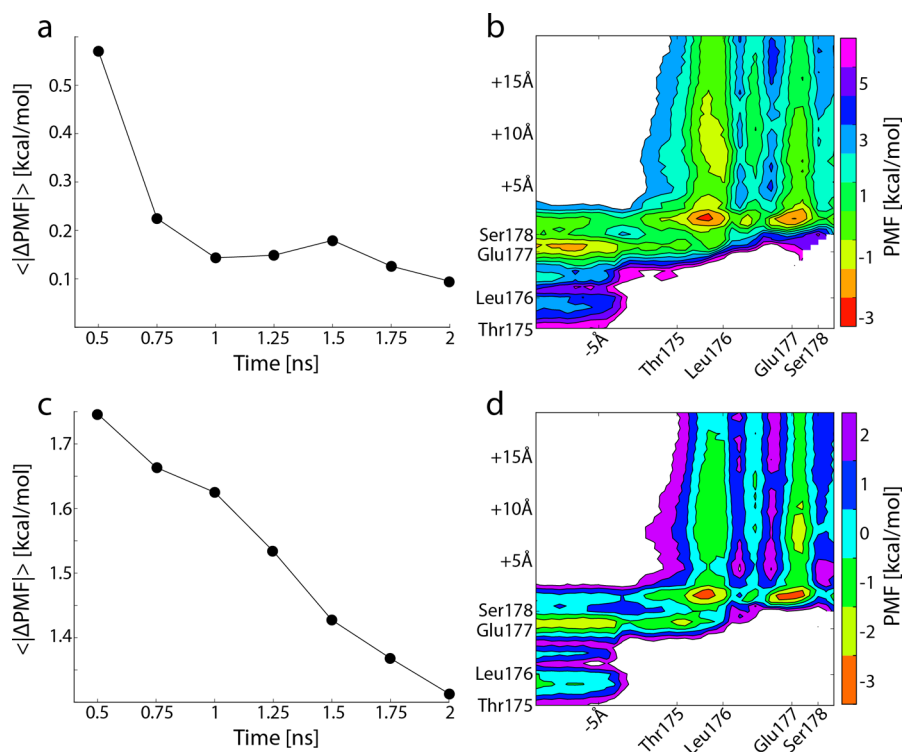


Figure 4. PMF estimated by US simulations. (a) Average difference between successive PMF estimates with US simulations of increasing length. The value at 500 ps corresponds to the average difference between the PMF maps calculated with US trajectories of respectively 500 and 250 ps. (b) PMF map calculated with US trajectories of 500 ps. (c) Average difference between the PMF map as calculated with US simulations of increasing length and the PMF map calculated by the BE-meta simulation BE_2NA. (d) PMF map calculated with US trajectories of 2.1 ns, with the first 0.7 ns discarded as equilibration time. All the differences between PMF maps were calculated after superimposing the two energy profiles.

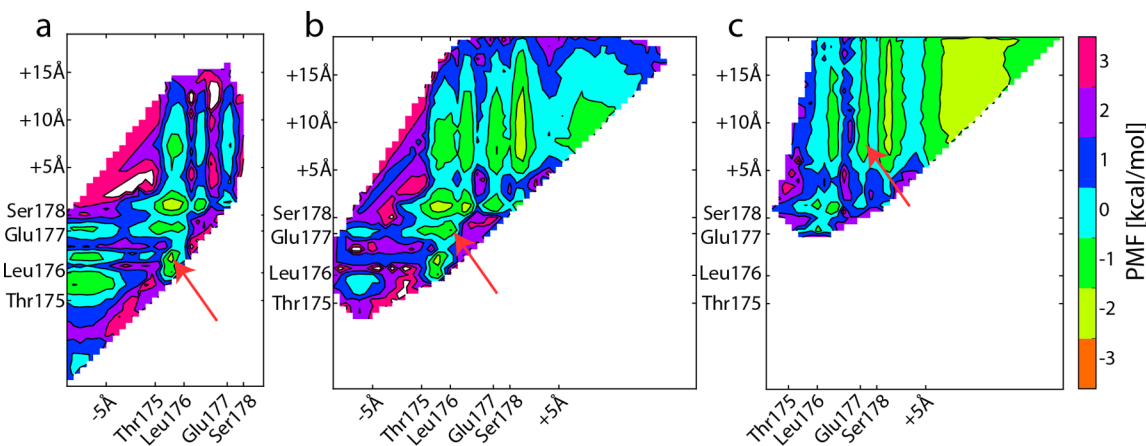


Figure 5. PMF in a BE-meta simulation with four Na^+ ions. The PMF was calculated with the WHAM algorithm, using data from the BE-meta simulation with four biased Na^+ ions in the time interval 96–192 ns. The 4-dimensional PMF profile was projected along the CV values of the innermost ions (a), middle ions (b), and outermost ions (c). Labels along the axes indicate the average positions of the carbonyl oxygens of residues Thr175, Leu176, and Ser178 and of the side chain oxygen atoms of residues Glu177. Displacements of -5 Å with respect to Thr175 (intracellular side of the selectivity filter) and $+5$ Å, $+10$ Å, and $+15$ Å with respect to Ser178 (extracellular side of the selectivity filter) are also shown. Contour lines are drawn every 1 kcal/mol. The red arrow indicates the position of the energy minimum $S_{\text{CEN}}/S_{\text{CEN}}/S_{\text{HFS}}/\text{OUT}$.

required for the BE-meta simulation BE_2NA (3 replica of 100 ns). The difference between successive PMF estimates decreases to ~ 0.1 kcal/mol with US simulations of 1 ns, a drift that is still present when simulations of 1.75 and 2.0 ns are compared. Figure 4c shows the average difference between the PMF map calculated by US with simulations of increasing length and the map calculated by the BE-meta simulation BE_2NA (ΔPMF in the 2-dimensional space is shown in Figure S3 of the Supporting Information). This difference

decreases linearly as the length of the US simulations is increased. The presence of a long-lasting drift in the PMF estimates (Figure 4a) and the linear convergence toward the BE-meta map (Figure 4c) suggest that the equilibration interval considered in the US trajectories (100 ps) was actually not sufficient to reach equilibration. In agreement with this hypothesis, the energy map calculated by US converged (± 1 kcal/mol) to the one calculated by the BE-meta simulation

BE_2NA when the first 700 ps of each trajectory were discarded (Figure 4d).

Simulations with 4 Na⁺ Ions. In the BE-meta simulation with four Na⁺ ions, the biasing potentials of the four replicas converged to a profile similar to the one observed in the BE-meta simulation with two ions (Figure 2). The time needed to fully sample the range of the CV values in all the replicas was 96 ns, almost double the time needed with two replicas. However, the PMF profile was statistically identical to the one estimated in the BE-meta simulation with two Na⁺ ions. This similarity suggests that simulations with two ions already captured the main features of the permeation process.

In order to reveal if states with three or four ions inside the pore are accessible, the PMF in this 4-dimensional space (variables CV of four Na⁺ ions) was calculated. Figure 5 shows the projections of the 4-dimensional PMF profile over the two innermost ions, the two ions in the middle, and the outermost ions. Although these projections are not straightforward to interpret, several energy minima with more than two ions inside the pore can be described (e.g., red arrow in Figure 5). The number of ions inside the selectivity filter affects the configuration of the glutamate residues E177 (Figure S4 in the Supporting Information). When the selectivity filter is occupied by two Na⁺ ions, the carbonyl oxygens of E177 are predominantly directed toward the extracellular side of the channel, while configurations with the carbonyl oxygen atoms pointing to the pore lumen are unlikely. The probability of the latter configuration increases when the filter is populated by 3 Na⁺ ions. In order to reach an intuitive view of the 4-dimensional PMF profile, the local energy minimum and the energy barriers between them were identified by an analysis based on KMC simulations (Figure 6). The configuration with two ions in S_{CEN}, one ion in S_{HFS}, and one ion in the extracellular compartment (S_{CEN}/S_{CEN}/S_{HFS}/OUT, configuration with green background at the bottom of Figure 6) corresponds to the global energy minimum. The equivalent configuration with three ions in the pore and the fourth ion in the intracellular compartment is 0.4 kcal/mol higher in energy (IN/S_{CEN}/S_{CEN}/S_{HFS}, configuration with green background at the top-right of Figure 6). Since a hydrated ion in the intracellular and the extracellular compartments is expected to be identical in energy, the difference between these two configurations defines a lower boundary for the uncertainty affecting the energy estimates.

Configurations S_{CEN}/S_{CEN}/S_{HFS}/OUT and IN/S_{CEN}/S_{CEN}/S_{HFS} can easily exchange with configurations with two ions inside the pore, owing to the exit of the outermost/innermost ion. When only two ions are inside the pore, the configurations with the lowest energies are the ones with one ion in S_{CEN} and one ion in S_{HFS} (IN/S_{CEN}/S_{HFS}/OUT and S_{CEN}/S_{HFS}/OUT/OUT, configurations with blue background in Figure 6). There are two possibilities to move from IN/S_{CEN}/S_{HFS}/OUT to S_{CEN}/S_{HFS}/OUT/OUT. Looking at conduction from the outward direction, one possibility (blue arrows in Figure 6) is that first the ion in S_{HFS} moves to the extracellular compartment, and then the two ions, in the intracellular compartment and S_{CEN}, move upward in a concerted manner reaching S_{CEN} and S_{HFS}. By an alternative route (red arrows in Figure 6), the ion in the intracellular compartment transits to S_{CEN} driving away the ions in S_{CEN} to S_{HFS}. The cycle is then completed by the exit of one of the two ions in S_{HFS} to the extracellular solution. The states with background of the same color in Figure 6 correspond to complete permeation events.

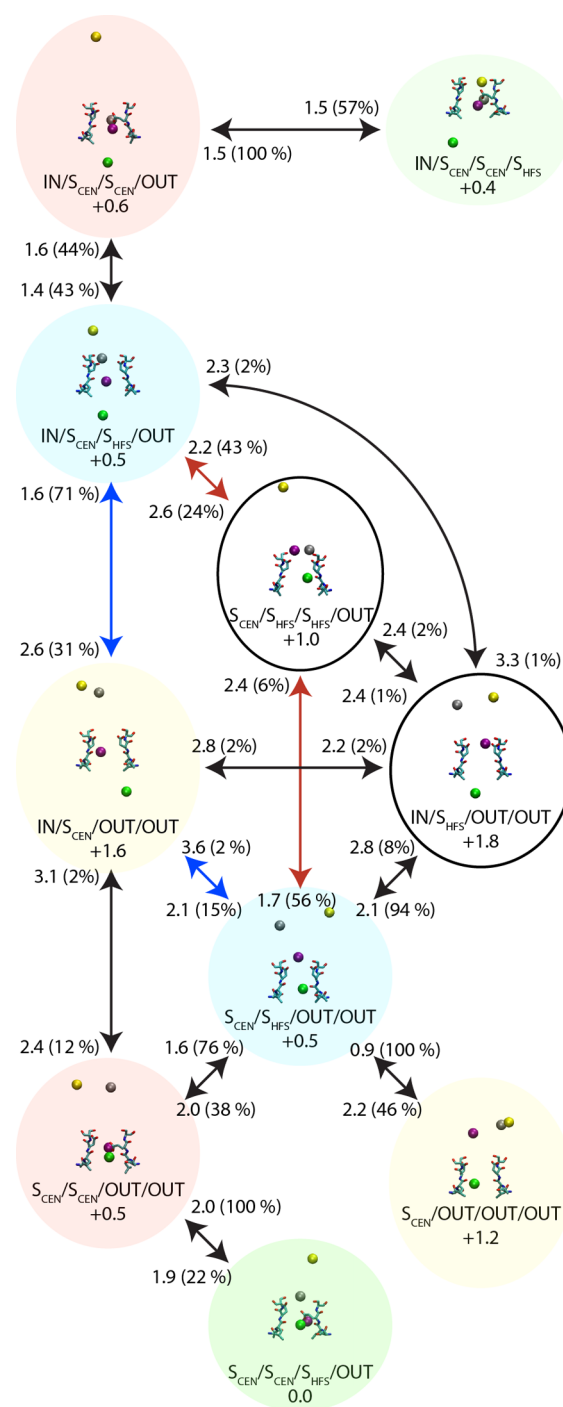


Figure 6. Energy minima in the 4-dimensional PMF. Snapshots of the selectivity filter are shown for all the local energy minima in the 4-dimensional PMF profile. The value of the energy in the local minima with respect to the global minimum (S_{CEN}/S_{CEN}/S_{HFS}/OUT) is shown below the label for each configuration. Ions are shown as colored VdW spheres, from the innermost to the outermost ions, in green, purple, gray, and yellow. Residues Thr175 to Ser178 of the selectivity filter are shown in licorice representation. Configurations with the same background color correspond to the final states of a complete permeation event, i.e. same occupancy of the selectivity filter and movement of one ion across the channel. The energy barriers for state transitions are shown adjacent to the corresponding arrows. The values in parentheses correspond to the probability of leaving a state along that particular direction in the KMC simulation.

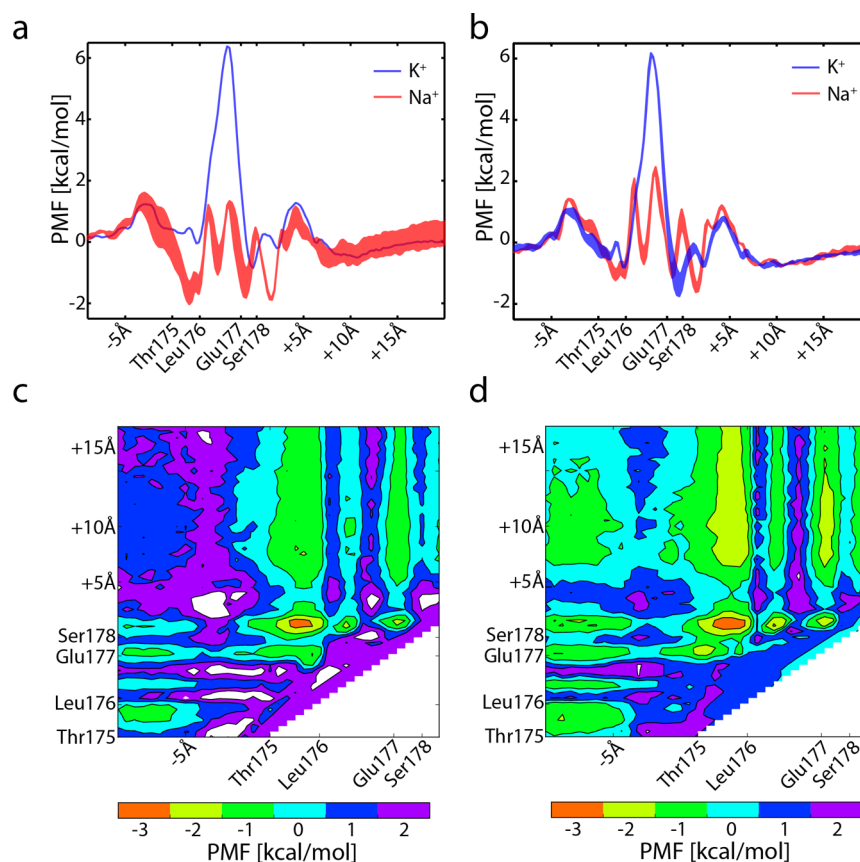


Figure 7. PMF in a BE-meta simulation with (i) two Na^+ ions and one K^+ ion (a-c) and (ii) two Na^+ ions and two K^+ ions (b-d). (a-b) 1-dimensional PMF profiles for Na^+ ions (red lines) and K^+ ions (blue lines) estimated from the simulations BE_2NA_1K (a) and BE_2NA_2K (b). (c-d) 2-dimensional PMF profiles for Na^+ ions. The 2-dimensional PMF maps for Na^+ ions were calculated by the WHAM algorithm, using respectively the data from the BE-meta simulation BE_2NA_1K in the time interval 136–272 ns (panel c), and from the BE-meta simulation BE_2NA_2K in the time interval 152–304 ns (panel d). Average positions of the carbonyl oxygen atoms of residues Thr175, Leu176, and Ser178 and of the side chain oxygen atoms of residues Glu177 are indicated. Displacements of -5 \AA with respect to Thr175 (intracellular side of the selectivity filter) and $+5 \text{ \AA}$, $+10 \text{ \AA}$, and $+15 \text{ \AA}$ with respect to Ser178 (extracellular side of the selectivity filter) are also shown. Contour lines are drawn every 1 kcal/mol .

The transition $\text{IN}/\text{S}_{\text{CEN}}/\text{OUT}/\text{OUT}$ (yellow background) \rightarrow $\text{S}_{\text{CEN}}/\text{S}_{\text{HFS}}/\text{OUT}/\text{OUT}$ (blue background) \rightarrow $\text{S}_{\text{CEN}}/\text{OUT}/\text{OUT}/\text{OUT}$ (yellow background) is analogous to the conduction event observed in the BE-meta simulation with only two biased Na^+ ions, with the only difference being that two extra ions are present in the extracellular compartment. Many other permeation routes with similar energy barriers can be observed in the 4-dimensional PMF profile. Therefore, several arrangements of ions can coexist during permeation, and the proposed approach based on BE-meta simulations facilitates the analysis of all these possibilities by employing a single set of simulations.

Simulations of Na^+/K^+ Ion Mixtures. The simulation protocol previously described can be applied also to the study of permeation properties of ion mixtures by biasing different types of ions in several replicas. Since the main features of Na^+ conduction were captured in the BE-meta simulation with two ions, this configuration was used to analyze the effects of the presence of K^+ ions. Two BE-meta simulations were performed: one with replicas with two Na^+ ions and one K^+ ion biased (BE_2NA_1K) and another with replicas with two Na^+ and two K^+ ions biased (BE_2NA_2K). In the case of mixtures, the equilibration time required was longer than in the simulations of Na^+ ions (136 and 152 ns in BE_2NA_1K and BE_2NA_2K, respectively). The central region of the pore is

a high-energy state for K^+ ions (Figure 7), and, consequently, higher biasing potentials and longer simulation times are required to sample the entire range of CV in the replicas where K^+ ions are biased. Interestingly, the 1-dimensional PMF profiles for Na^+ ions were identical to the ones estimated previously in BE-meta simulations with only Na^+ ions (compare Figure 7a-b and Figure 2). The same applies to the 2-dimensional PMF maps (compare Figure 7c-d and Figure 3). The similarity of PMF maps with and without K^+ ions reflects the fact that the presence of K^+ does not interfere in Na^+ permeation. The only noticeable difference is that in the BE-meta simulation with two K^+ ions, energy minima exist when both Na^+ ions are outside the pore. This configuration was not observed in the BE-meta simulation BE_2NA because the two Na^+ ions were the only cations that could penetrate the channel, and the high electronegative filter is unlikely to be completely depleted of positive charges. Instead, in simulations of mixtures, configurations with both Na^+ ions outside the pore are energetically accessible, as other cations such as K^+ ions can bind to the selectivity filter. The energy minima with both Na^+ ions outside the pore observed in the BE-meta simulation BE_2NA_2K (Figure 7d, $x < -5 \text{ \AA}$ and $y > +5 \text{ \AA}$) correspond to configurations with the filter occupied by K^+ ions. Remarkably, the energy of these minima is 2 kcal/mol higher than the minimal energy observed with Na^+ ions inside the

pore, proving that in the presence of Na^+/K^+ mixtures the pore still prefers Na^+ ions. The difference between K^+ and Na^+ ions can be ascribed to the fact that K^+ ions cannot bind in the region between Leu176 and Glu177, as shown by the 1-dimensional PMF profile. K^+ ions experience an energy barrier of ~ 6 kcal/mol in this central area of the pore, and as a consequence they are excluded from permeation events. It must be noted that by performing BE-meta simulations with Na^+/K^+ mixtures, it was possible to analyze the permeation properties and the selectivity mechanism using a single set of simulations.

DISCUSSION

The increasing availability of crystallographic structures of ion channels makes the development of efficient protocols and computational strategies to investigate their properties highly desirable. The approach that was tested in this study, based on BE-meta simulations, has turned out to be a promising alternative to US, the technique commonly employed to analyze conduction and selectivity by computer simulations. In this study, a converged estimate of the energy map for conduction of two Na^+ ions across a toy model of bacterial Na^+ channels was achieved by a BE-meta simulations of ~ 300 ns. In contrast, full energy convergence of the same process estimated from US was not achieved after $1 \mu\text{s}$.

Defining the precise number or type of ions that are involved in conduction is not essential in BE-meta simulations, and this is an advantage over US. Theoretically, even with US simulations (and also metadynamics or other free energy techniques) it is not strictly necessary to define in advance the number of permeating ions. One could accelerate the dynamics of a single permeating ion and wait for the other ions in the system to equilibrate. However, as described in the Introduction, this approach would require extremely long simulation times to achieve convergence. An alternative route to the unavoidable preliminary selection of the number of permeating ions in US or metadynamics simulations is to calculate the PMF map using a number of collective variables that exceeds the number of ions that are likely to be involved in conduction events. Once the energy map in this N -dimensional space is calculated, it will be possible to reveal the precise number of ions involved in conduction as well as the energetically accessible mechanisms of permeation. The drawback of this strategy is that the time needed to estimate a free energy map increases exponentially with the number of collective variables. As an example, more than 50,000 umbrella sampling trajectories would be necessary to analyze the 4-dimensional space defined by the axial-coordinates of four Na^+ ions across the NaVA channel, amounting to a total simulation time above $100 \mu\text{s}$ if trajectories of 2 ns are considered. Instead, with BE-meta, a total simulation time below $1 \mu\text{s}$ was sufficient to energetically illustrate the same process. This degree of efficiency is possible because each replica in a BE-meta simulation explores a 1-dimensional space, while sampling in the 4-dimensional space is accelerated by exchanges between replicas. The possibility to explore high-dimensional spaces with limited computational resources is extremely important for the analysis of ion channels, since it allows the simulation of multi-ion conduction events and ion mixtures.

The set of collective variables used in BE-meta simulations could easily be expanded to include variables that describe protein motions. In the case that the motion of the protein takes place in the same time scale of conduction events, accelerating the sampling of this collective variable might

improve the efficiency of PMF calculations by BE-meta simulations. Na^+ channels provide a possible example for this situation. Chakrabarti et al. observed two possible configurations for the glutamate residues of the selectivity filter: one with the side chain pointing to the extracellular side of the channel and another with the carbonyl oxygen atoms directed toward the pore lumen.¹⁴ These two configurations were observed to exchange with transition-rates on the same time scale of the ion movements across the selectivity filter. In agreement with the results of Chakrabarti et al.,¹⁴ the same two configurations were observed in the BE-meta simulation with four Na^+ ions, and the probability of the configuration with the side chain directed to the pore axis increased for higher ion-occupancies of the selectivity filter. This qualitative agreement reflects the fact that the atomic system used in this study offers a satisfactory model for the selectivity filter of a Na^+ channel. However, a quantitative analysis of the structural changes in the selectivity filter requires the usage of an atomic model of the entire Na^+ -channel. BE-meta simulations are a promising strategy to analyze how structural changes of the selectivity filter modifies the conduction properties and consequently to fully characterize the behaviors of the glutamate residues in the selectivity filter of Na^+ channels.

An alternative approach to free-energy calculations for the study of ion channels is the simulation of conduction using classical MD simulations.^{14,33–37} This approach has become popular for two main reasons. First, simulations in the microsecond time scale do not require dedicated architectures anymore, and second, algorithms have been developed to simulate gradients across cell membrane in MD simulations with periodic boundary conditions,^{38–40} where events are pinpointed as they happen. MD simulations with a membrane potential applied across the cell membrane have one major advantage over free-energy methods: they allow for directly estimating the I–V curve of an ion channel. This strategy has been applied to analyze conduction in the NaVMs Na^+ -channel, obtaining a good agreement with experimental data.⁴¹ In these “brute-force” MD simulations, the correct permeation kinetics is preserved, while these properties are not directly accessible in simulations where biasing potentials are used to “accelerate” sampling. Nevertheless, free-energy calculations can be combined with the electrodiffusion theory to estimate the channel conductance.⁴² Moreover, studies based on free-energy algorithms are more efficient than brute-force simulations providing that the right set of collective variables is chosen. The protocol tested in this study alleviates some of the issues inherited in the choice of the collective variables required to study conduction. BE-meta has emerged as a powerful strategy in the computational study of membrane proteins.

ASSOCIATED CONTENT

Supporting Information

Figure S1, model system; Figure S2, difference between PMF maps estimated with umbrella sampling simulations of different length; Figure S3, difference between PMF maps estimated with BE-meta simulations and with umbrella sampling simulations of different length; Figure S4, configurations of residues E177. This material is available free of charge via the Internet at <http://pubs.acs.org>.

AUTHOR INFORMATION

Corresponding Author

*Phone: 390577585730. E-mail: simone.furini@unisi.it.

Notes

The authors declare no competing financial interest.

ACKNOWLEDGMENTS

This work was supported by a CINECA Award under the ISCRA initiative. C. Domene would like to acknowledge the use of computational resources from the EPSRC UK National Service for Computational Chemistry Software (NSCCS), Archer and the Hartree Center.

REFERENCES

- (1) Doyle, D. A.; Cabral, J. M.; Pfuetzner, R. A.; Kuo, A.; Gulbis, J. M.; Cohen, S. L.; Cahit, B. T.; MacKinnon, R. The structure of the potassium channel: molecular basis of K^+ conduction and selectivity. *Science* **1998**, *280*, 69–77.
- (2) Payandeh, J.; Scheuer, T.; Zheng, N.; Catterall, W. A. The crystal structure of a voltage-gated sodium channel. *Nature* **2011**, *475*, 353–358.
- (3) Furini, S.; Domene, C. K^+ and Na^+ conduction in selective and nonselective ion channels via molecular dynamics simulations. *Biophys. J.* **2013**, *105*, 1737–1745.
- (4) Berneche, S.; Roux, B. Energetics of ion conduction through the K^+ channel. *Nature* **2001**, *414*, 73–77.
- (5) Furini, S.; Domene, C. Atypical mechanism of conduction in potassium channels. *Proc. Natl. Acad. Sci. U. S. A.* **2009**, *106*, 16074–16077.
- (6) Corry, B.; Thomas, M. Mechanism of ion permeation and selectivity in a voltage gated sodium channel. *J. Am. Chem. Soc.* **2012**, *134*, 1840–1846.
- (7) Fowler, P. W.; Abad, E.; Beckstein, O.; Sansom, M. S. Energetics of Multi-Ion Conduction Pathways in Potassium Ion Channels. *J. Chem. Theory Comput.* **2013**, *9*, 5176–5189.
- (8) Thompson, A. N.; Kim, I.; Panosian, T. D.; Iverson, T. M.; Allen, T. W.; Nimigean, C. M. Mechanism of potassium-channel selectivity revealed by Na^+ and Li^+ binding sites within the KcsA pore. *Nat. Struct. Mol. Biol.* **2009**, *16*, 1317–1324.
- (9) Stock, L.; Delemotte, L.; Carnevale, V.; Treptow, W.; Klein, M. L. Conduction in a biological sodium selective channel. *J. Phys. Chem. B* **2013**, *117*, 3782–3789.
- (10) Henin, J.; Tajkhorshid, E.; Schulten, K.; Chipot, C. Diffusion of glycerol through Escherichia coli aquaglyceroporin GlpF. *Biophys. J.* **2008**, *94*, 832–839.
- (11) Ngo, V.; Stefanovski, D.; Haas, S.; Farley, R. A. Non-Equilibrium Dynamics Contribute to Ion Selectivity in the KcsA Channel. *PLoS One* **2014**, *9*.
- (12) Hodgkin, A. L.; Keynes, R. D. The potassium permeability of a giant nerve fibre. *J. Physiol.* **1955**, *128*, 61–88.
- (13) Furini, S.; Domene, C. On conduction in a bacterial sodium channel. *PLoS Comput. Biol.* **2012**, *8*, e1002476.
- (14) Chakrabarti, N.; Ing, C.; Payandeh, J.; Zheng, N.; Catterall, W. A.; Pomes, R. Catalysis of Na^+ permeation in the bacterial sodium channel NaVA. *Proc. Natl. Acad. Sci. U. S. A.* **2013**, *110*, 11331–11336.
- (15) Ke, S.; Timin, E. N.; Stary-Weinzinger, A. Different Inward and Outward Conduction Mechanisms in NaVMs Suggested by Molecular Dynamics Simulations. *PLoS Comput. Biol.* **2014**, e1003746.
- (16) Piana, S.; Laio, A. A bias-exchange approach to protein folding. *J. Phys. Chem. B* **2007**, *111*, 4553–4559.
- (17) Laio, A.; Parrinello, M. Escaping free-energy minima. *Proc. Natl. Acad. Sci. U. S. A.* **2002**, *99*, 12562–12566.
- (18) Pronk, S.; Pall, S.; Schulz, R.; Larsson, P.; Bjelkmar, P.; Apostolov, R.; Shirts, M. R.; Smith, J. C.; Kasson, P. M.; van der Spoel, D.; et al. GROMACS 4.5: a high-throughput and highly parallel open source molecular simulation toolkit. *Bioinformatics* **2013**, *29*, 845–854.
- (19) MacKerell, A. D.; Bashford, D.; Bellott, M.; Dunbrack, R. L.; Evanseck, J. D.; Field, M. J.; Fischer, S.; Gao, J.; Guo, H.; Ha, S.; et al. All-Atom Empirical Potential for Molecular Modeling and Dynamics Studies of Proteins. *J. Phys. Chem. B* **1998**, *102*, 3586–3616.
- (20) Jorgensen, W. L.; Chandrasekhar, J.; Madura, J. D.; Impey, R. W.; Klein, M. L. Comparison of Simple Potential Functions for Simulating Liquid Water. *J. Chem. Phys.* **1983**, *79*, 926–935.
- (21) Beglov, D.; Roux, B. Finite Representation of an Infinite Bulk System: Solvent Boundary Potential for Computer Simulations. *J. Chem. Phys.* **1994**, *100*, 9050–9063.
- (22) Bussi, G.; Donadio, D.; Parrinello, M. Canonical sampling through velocity rescaling. *J. Chem. Phys.* **2007**, *126*, 014101.
- (23) Parrinello, M.; Rahman, A. Polymorphic transitions in single-crystals - a new molecular-dynamics method. *J. Appl. Phys.* **1981**, *52*, 7182–7190.
- (24) Essmann, U.; Perera, L.; Berkowitz, M. L.; Darden, T.; Lee, H.; Pedersen, L. G. A smooth particle mesh Ewald method. *J. Chem. Phys.* **1995**, *103*, 8577–8593.
- (25) Hess, B.; Bekker, H.; Berendsen, H. J. C.; Fraaije, J. LINCS: A linear constraint solver for molecular simulations. *J. Comput. Chem.* **1997**, *18*, 1463–1472.
- (26) Bonomi, M.; Branduardi, D.; Bussi, G.; Camilloni, C.; Provasi, D.; Raiteri, P.; Donadio, D.; Marinelli, F.; Pietrucci, F.; Broglia, R. A.; et al. PLUMED: A portable plugin for free-energy calculations with molecular dynamics. *Comput. Phys. Commun.* **2009**, *180*, 1961–1972.
- (27) Marinelli, F.; Pietrucci, F.; Laio, A.; Piana, S. A kinetic model of trp-cage folding from multiple biased molecular dynamics simulations. *PLoS Comput. Biol.* **2009**, *5*, e1000452.
- (28) Kumar, S.; Bouzida, D.; Swendsen, R. H.; Kollman, P. A.; Rosenberg, J. M. The weighted histogram analysis method for free-energy calculations on biomolecules. 1. The method. *J. Comput. Chem.* **1992**, *13*, 1011–1021.
- (29) Gillespie, D. T. A general method for numerically simulating the stochastic time evolution of coupled chemical reactions. *J. Comput. Phys.* **1976**, *22*, 403–434.
- (30) Hummer, G. Position-dependent diffusion coefficients and free energies from Bayesian analysis of equilibrium and replica molecular dynamics simulations. *New J. Phys.* **2005**, *34*.
- (31) Nelder, J. A.; Mead, R. A Simplex Method for Function Minimization. *Comput. J.* **1965**, *7*, 308–313.
- (32) Furini, S.; Barbini, P.; Domene, C. Effects of the protonation state of the EEEE motif of a bacterial Na^+ -channel on conduction and pore structure. *Biophys. J.* **2014**, *106*, 2175–83.
- (33) Khalili-Araghi, F.; Tajkhorshid, E.; Schulten, K. Dynamics of K^+ ion conduction through Kv1.2. *Biophys. J.* **2006**, *91*, L72–74.
- (34) Jensen, M. O.; Jogini, V.; Eastwood, M. P.; Shaw, D. E. Atomic-level simulation of current-voltage relationships in single-file ion channels. *J. Gen. Physiol.* **2013**, *141*, 619–632.
- (35) Domene, C.; Sansom, M. S. P. Potassium channel, ions, and water: Simulation studies based on the high resolution X-ray structure of KcsA. *Biophys. J.* **2003**, *85*, 2787–2800.
- (36) Domene, C.; Vemparala, S.; Furini, S.; Sharp, K.; Klein, M. L. The role of conformation in ion permeation in a K^+ channel. *J. Am. Chem. Soc.* **2008**, *130*, 3389–3398.
- (37) Aksimentiev, A.; Schulten, K. Imaging alpha-hemolysin with molecular dynamics: ionic conductance, osmotic permeability, and the electrostatic potential map. *Biophys. J.* **2005**, *88*, 3745–3761.
- (38) Khalili-Araghi, F.; Ziervogel, B.; Gumbart, J. C.; Roux, B. Molecular dynamics simulations of membrane proteins under asymmetric ionic concentrations. *J. Gen. Physiol.* **2013**, *142*, 465–475.
- (39) Gumbart, J.; Khalili-Araghi, F.; Sotomayor, M.; Roux, B. Constant electric field simulations of the membrane potential illustrated with simple systems. *Biochim. Biophys. Acta* **2012**, *1818*, 294–302.
- (40) Kutzner, C.; Grubmüller, H.; de Groot, B. L.; Zachariae, U. Computational electrophysiology: the molecular dynamics of ion channel permeation and selectivity in atomistic detail. *Biophys. J.* **2011**, *101*, 809–817.
- (41) Ulmschneider, M. B.; Bagneris, C.; McCusker, E. C.; Decaen, P. G.; Delling, M.; Clapham, D. E.; Ulmschneider, J. P.; Wallace, B. A. Molecular dynamics of ion transport through the open conformation of a bacterial voltage-gated sodium channel. *Proc. Natl. Acad. Sci. U. S. A.* **2013**, *110*, 6364–6369.

(42) Berneche, S.; Roux, B. A microscopic view of ion conduction through the K⁺ channel. *Proc. Natl. Acad. Sci. U. S. A.* **2003**, *100*, 8644–8648.